Journal of Materials and Engineering Structures

Research Paper

Simulation of Border Deformation in Corrosion System by Coupling Analytical Solution and Finite Element Method

Djedjiga Boukhlef [a,*], ***Dalila Boughrara*** [b], ***Hassane Mohellebi*** [c]

[a] *Unité de Recherche en Energies Renouvelables en Milieu Saharien, URERMS, Centre de Développement des Energies Renouvelables, CDER, (01000), Adrar, Algeria*

[b] *Physics and Chemistry of Materials Laboratory, UMMTO, Tizi-Ouzou, Algeria*

[c] *Numerical Modeling of Electromagnetic Phenomenon and Components Laboratory, UMMTO, Tizi-Ouzou, Algeria.*

ARTICLE INFO

Article history :

Received : 28 January 2018

Revised : 30 May 2018

Accepted : 28 June 2018

Keywords:

Coupling anlytical

Finite Element Method

Boudary deformation

ABSTRACT

The objective of this work is to develop a digital model in order to envisage metal degradation on a microscopic scale. The reaction on the surface of the anodic considered as a degradation reaction when the surface forming the cathode remains unchanged. A one dimensional analytical solution representing the two mediums (anode and cathode), is introduced in the form of boundary conditions of Neumann type to the interface metal/electrolyte and thus the resolution was performed without mesh the analytical zone. Also, no re-meshing solving domain was need when simulating the border deformation.

1 Introduction

The Al-Mg alloys are widely used on the cabin of ships, vehicles, aerospace and maritime structures, for its lightness, low weight, best combination of high strength with corrosion resistance, ductility, good weldability (for level < 3% Mg). However, it is sensitive to different types of surface damage, for reasons of corrosion or degradation when they are in physical contact with other metals. This phenomenon alters the material properties and leads to undesirable economic consequences.

Galvanic corrosion occurs between two metals of different corrosion potentials, immersed in the same electrolyte and electrically connected. The potential difference called driving force causes a flow of current called galvanic current.

* *Corresponding author.*
E-mail address: boukhlefdjidji@urerms.dz

e-ISSN: 2170-127X,

RESEARCH REVIEW of Sciences and Technologies

Consequently, the corrosion rate of the more noble (positive) material, called the cathode, decreases or suppress, while it increases for the more negative one, called the anode. Small surface area of anodic material compared to cathodic material close together is a good indicator for galvanic corrosion. This phenomena is desirable in many engineering applications, particularly in cathodic protection [1, 2].

Galvanic corrosion has been widely studied experimentally and by numerical modeling and few works has been made to verify the agreement between them [3-6]. However, it is very hard to experimentally evaluate the galvanic corrosion process of steel structure in atmosphere from experiments in a laboratory where different factors cannot be taken into account such loading density, relative humidity, area ratio of metals, thickness of electrolyte and so on [7]. That is why computational modeling is considered as an effective tool to predict atmospheric corrosion.

Theoretical studies have been reported first by Wagner [8] assuming a linear polarization law on the anode-cathode couple, and indicating a degree of current uniformity on an anode, but does not predicts the current and potential distributions. Waber [9, 10] introduced equal constant polarization parameters of linear corrosion kinetics which have been extended by McCaferty [11] with unequal constant polarization parameters. Waber and McCaferty reported that local current densities of the anode oxidation and the cathode reduction increase with increasing electrolyte thickness. Numerical models have been proposed by other authors that introduced a diffusion limited process of oxygen cathodic reaction in the electrode kinetics to investigate the influence of electrolyte thickness, conductivity and defect on the couple interface beneath a thin layer of electrolyte [5, 6, 12, 13], but to our knowledge only Lee [12] considered a diffusion limited process for oxygen cathodic reaction, which is the most susceptible to occur in near neutral solution. In the model proposed in [5], standard equations for the electrochemical kinetic of electrochemical couples have been chosen. This methodology allows changing the galvanic cell geometry, as electrolyte thickness, in keeping same boundaries conditions [12, 14]. This provides a great flexibility of the model to different galvanic corrosion situations like corrosion under a thin electrolyte layer. Jorcin et al [15] have reported a galvanic corrosion study of Al/Cu couple with a fixed value of anodic current on Al and a cathodic current function of local potential on Cu as boundary conditions. They indicate an increase of the oxygen reduction current from the initial immersion time. Simulation of galvanic corrosion between magnesium and aluminium has been performed by Lacroix et al. [16]. Deshpande [4, 16, 17], Jia et al. [19], and Trinh et al. [20] have studied the corrosion of magnesium alloys in contact to mild steel. The publications of Murer et al. [1, 2, 21] and Shi and Kelly [22] in this context also gave an extended insight into the topic, especially in the very important choice of boundary conditions in Comsol. Oltra et al [23] built a model to predict the potential and the current density distribution of aluminum alloy-steel galvanic couple under thin electrolyte.

New studies of Sun et al. [24] applied the mathematical approach of Yan et al [25] to the modeling of deposit formation under seawater conditions, clearly introduce a possible way of a useful model built up for the mentioned purpose. The following studies and results are based on the progress achieved by them. Basic galvanic current density computations were modified by layer growth aspects leading to time dependent variations in the electrochemical response of the electrodes [26].

The main objective of this study is to develop a numerical model in order to predict the metal degradation [27]. In the model time calculation is varied and associated to the anode surface degradation when coupled to the cathode surface which remains unchanged. The two mediums in contact are represented by a one dimensional (1D) analytical solution. This solution is introduced as Neumann boundary conditions at the metal/electrolyte interface .The physical problem is addressed by the finite element method by combining the partial differential equation of electric conduction to the deformation of the mesh by considering the motion of the boundary of the degraded surface. This model is based on data obtained from non-linear polarization measurements and allows tracking the interface which degrades. Gauss-Newton algorithm is used for solving the non linear model and boundary element method are employed for the numerical calculation [24].

2 Experimental

This part was carried out in order to determine the kinetic parameters that must be inserted as boundary conditions in the model of the COMSOL software.

Test specimens of Al-2.5 wt. % Mg alloy and steel are employed for polarization curves measurements. Prior to any test the metallic surface of the specimens is mechanically polished on a range of silicon carbide paper up to 2000 grit under

water jet, followed by polishing on felt soaked with alumina in suspension in water then cleaned under ultrasonic in ethanol and finally rinsed with distilled water.

The experimental potentiodynamic polarization curves are plotted on both Al-Mg alloy and steel plates separately in 3 wt.% NaCl solution, having a conductivity of 6 S/m and a pH value of 6.5 and ambient temperature (20 ± 2°C) (Fig. 1). The scans are started from cathodic potential and swept in the positive direction at a scan rate of 1 mV/s. The speed is slower and gives better and reproducible results. The setup used the reference electrode (RE) of Ag-AgCl with the counter electrode of platinum plate, directly immersed in the electrolyte. The curves are recording using a potentiostat galvanostat.

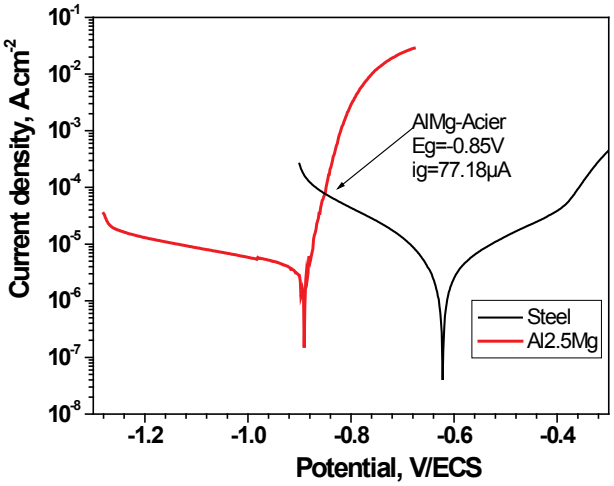

Fig. 1 – Experimental polarization curves after 1 h of immersion in 3wt. % NaCl at 1 mV/s

The polarization curves exhibit linear slopes on semi-logarithmic scale (i.e., Tafel slope) from 50 to 100 mV away from the corrosion potential.

The following reactions are considered here. Knowing that corrosion potential of Al-Mg is more anodic then steel, it will form the anode during galvanic coupling to steel, and it will dissolve:

$$Al \rightarrow Al^{3+} + 3e^- \quad (1)$$

$$Mg \rightarrow Mg^{2+} + 2e^- \quad (2)$$

While, the steel surface is the cathode where the dissolved oxygen (in alkaline aerated electrolyte) or the water reductions will take place for low and high overvoltage, respectively:

$$O_2 + 2H_2O + 4e^- \rightarrow 4OH^- \quad (3)$$

$$2H_2O + 2e^- \rightarrow H_2 + 2OH^- \quad (4)$$

The corrosion parameters of a material were obtained by extrapolating the linear portions of the polarization curves found at potentials well away from the corrosion potential (> 100 mV). The corrosion current density was determined from the intersection of the Tafel slopes at the corrosion potential. The coupling potential (E_{coup}) and the galvanic current density (i_g) are determined from the intersection of the anodic curve of the less noble material and the cathodic curve of the more noble material, according to the mixed potential method. All the kinetic parameters were used in the developed numerical model. Table 1 summarizes the constant values used in the model.

The Al-Mg sample has the more cathodic potential with a lower anodic Tafel slope which informs about the strong activation of its surface compared to Steel thus has the anodic corrosion potential, subject to a reduction reaction (3 or 4) when coupled to the alloy.

3 Numerical model

The model of AlMg-Steel galvanic couple has been previousely described [28]. The calculations were performed by exploiting the COMSOL Multiphysics software for the resolution. The dynamic model considered here uses the Conductive

Media DC and Moving Mesh (Arbitrary Lagrangian Eulerian: ALE) methods to track the border deformation (interface metal/solution).

Due to the system symmetry, the model implies a 2D geometry, configured in COMSOL Multiphysics as a 2D Axisymmetric model. Fig. 2 shows the geometry and the boundary conditions, which consist of axial symmetry, Steel and Al-Mg coplanar electrodes of the same size (0.25 cm) surrounded by insulating walls corresponding to the resin. The internal domain corresponds to the electrolyte with a defined value of thickness z = 1 cm giving a square area of 1 cm of side. The upper boundary is then far from electrode boundaries with a no-flux condition so the air-electrolyte surface can be modeled as an insulator. The 3 wt. % NaCl electrolyte is considered as homogeneous with a constant ohmic conductance (6 S/m). In this domain the governing equation of electric conduction for the current conservation and for the electric potential (in volts) distribution in the electrolyte surrounding the two metal surfaces, is the Laplace equation:

$$-\nabla.\left(\sigma\nabla\varphi\right)=0 \tag{1}$$

where σ is the electrical conductivity of the electrolyte and ϕ the electrical potential in the electrolyte.

When the electrical conductivity σ is considered constant, this equation is expressed in cylindrical co-ordinates and by using Galerkin method, the finite elements formulation becomes as follows [29]:

$$\iint_{\Omega} -\nabla\left(\sigma\nabla\varnothing\right)\alpha_j.d\Omega=0 \tag{2}$$

$$\begin{aligned}&\iint_{\Omega}\left[\left(-\frac{\partial}{\partial r}\left(\frac{\sigma}{r}\frac{\partial\Phi}{\partial r}\right)-\frac{\partial}{\partial z}\left(\frac{\sigma}{r}\frac{\partial\Phi}{\partial z}\right)\right)\alpha_j\right].drdz=\\&-\iint_{\Omega}\sigma\left[\left(\frac{\partial\Phi}{\partial r}\frac{\partial\alpha_j}{\partial r}\right)+\left(\frac{\partial\Phi}{\partial z}\frac{\partial\alpha_j}{\partial z}\right)\right].\frac{drdz}{r}-\int_{\Gamma}\sigma\left(\frac{\partial\Phi}{\partial r}n_r+\frac{\partial\Phi}{\partial z}n_z\right)\alpha_j\frac{d\Gamma}{r}=0\end{aligned} \tag{3}$$

With:

$$\Phi(r,z)=r\varphi(r,z) \tag{4}$$

$$\Phi(r,z)=\sum_{i=1}^{N}\alpha_i(r,z)\Phi_i \tag{5}$$

α_i : finite elements function called form function, Φ_i the nodal unknown at node i of the electric potential,

α_j: projection function which is considered the same one as finite elements function α_i,

n_r and n_z : are the normal vectors units along r and z coordinates respectively,

N: total number of nodes at the solving domain.

Ohm's law is used to express the current density J as a function of electrical potential gradient by the following formula:

$$J=-\sigma\frac{\partial\varphi}{\partial z} \tag{6}$$

Laplace's equation is solved in the electrolyte domain with the boundary conditions as represented in Fig. 2.

The kinetics at the metal / electrolyte interface, considered by the experimental data obtained from the polarization curves of the individual materials (Fig. 1), are used as boundary condition for the anode and the cathode surfaces and are introduced through the Neumann boundary conditions called "Inward current density" in COMSOL Multiphysics software [4, 23, 30]:

$$-n.J=J_n\left(\phi\right) \tag{7}$$

With n is the normal vector to the boundary, the function J_n (ϕ) shows the nonlinear polarization curve of the anode or cathode, expressed by exponential relations between the current density and the electrode potential: Eq. (8) and (9) for reactions (1-2) and (3-4), respectively:

$$J_n(\phi) = \begin{cases} -J_a(\phi) = -i_{corr,a}\, exp\left(\alpha_a\left(\phi - E_{corr,a}\right)\right) & \text{Dissolution of AlMg} \\ -J_c(\phi) = i_{corr,c}\, exp\left(-\beta_c\left(\phi - E_{corr,c}\right)\right) & \text{Reduction of the Steel} \end{cases} \quad (8, 9)$$

Where $i_{corr,a}$ and $i_{corr,c}$ are the corrosion current densities, $E_{corr,a}$ and $E_{corr,c}$ the corrosion potentials, $\alpha_a = 2.303/b_a$ and $\beta_c = 2.303/b_c$ the coefficient of Tafel slopes of the Al-Mg anode and the Steel cathode, respectively.

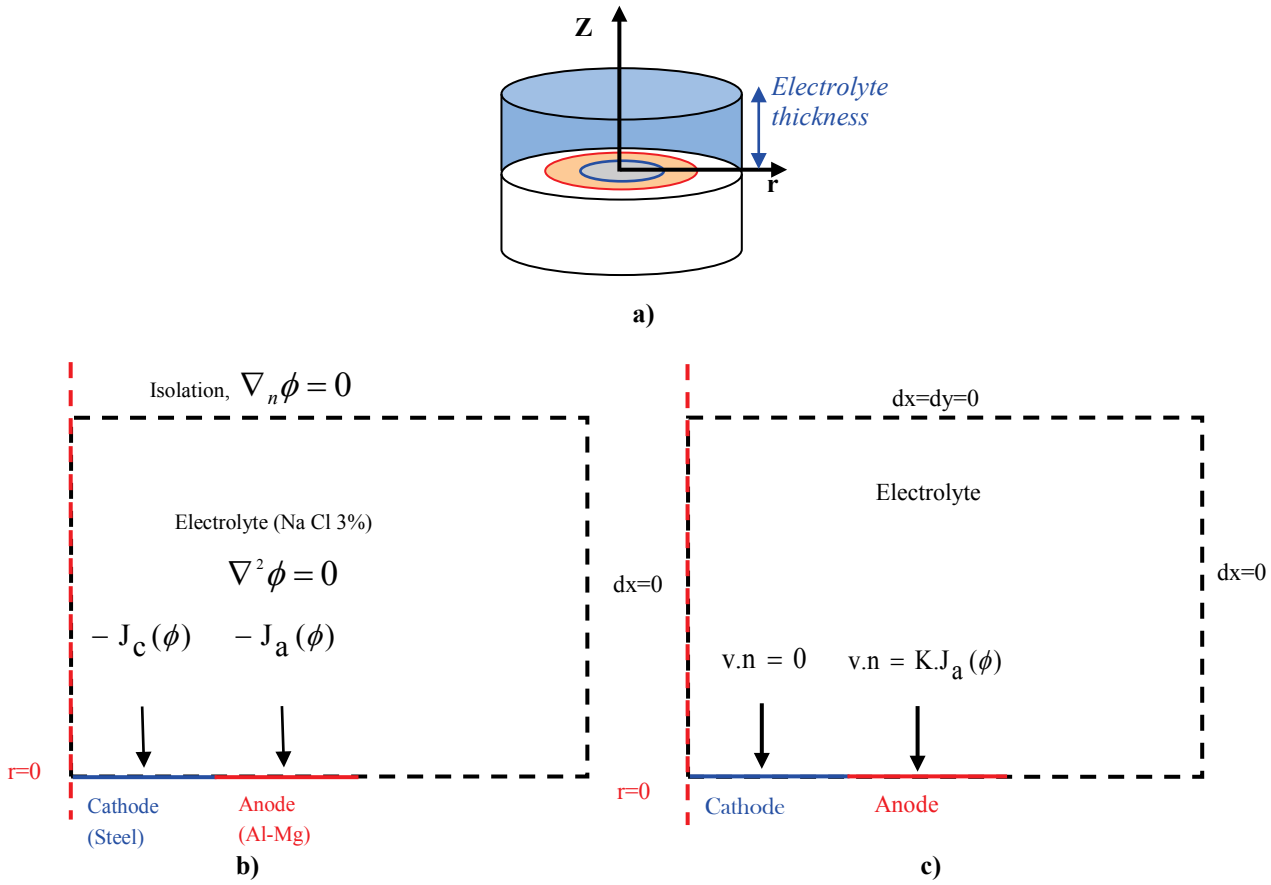

Fig. 2 – a) 2D geometry of the system and boundary conditions b) Conduction problem, c) Geometry deformation problem

The boundary condition imposed on the other boundaries is electrical insulation:

$$\nabla_n\varphi = 0 \quad \text{ou} \quad n.J(\phi) = 0 \quad (10)$$

The "Arbitrary Lagrangian Eulerian (ALE)" method is used for taking account of the change in geometry (displacement of the border). The ALE frame comprises a spacial frame with co-ordinates moving with time for the 2D geometry.

The rate of the mesh normal to the surface of the anode which dissolves becomes [4]:

$$v.n = -K\, J_n(\phi) \quad (11)$$

where $\boldsymbol{n}$ is normal component of velocity vector $\boldsymbol{v}$, K is the coefficient of proportionality, equal to 3.45 10^{-11} $C^{-1}.m^3$. It is calculated from the following equation:

$$K = \frac{M_{Al}}{zF\rho_{Al}} \quad (12)$$

where z is a reaction valence (or the electron number) equal to 3 for Al, F is the Faraday constant (96485 C/mol), M_{Al} is the molar mass (27 g/mol for Al), ρ_{Al} is density equal to 2.7 g/cm^3 for Al. In the SI units K = 3.45 10^{-11} C^{-1}.m^3. It is found to be 3.45 10^{-11} C^{-1}.m^3 for silicon [31].

As the surface of the cathode remains unchanged, the mesh rate at the cathode is zero.

Table 1- Input constant values used in the model

Property with units	Value
b_a (V/dec): Anodic Tafel slope of Al-2.5Mg	0.03
b_c (V/dec): Cathodic Tafel slope of Steel	- 0.135
Corrosion potential $E_{corr,a}$ (V/ECS) of Al-2.5Mg	- 0.890
Corrosion potential $E_{corr,c}$ (V/ECS) of Steel	- 0.622
Corrosion Current density $i_{corr,a}$ (A/m^2) of Al-2.5Mg	0.04
Corrosion Current density $i_{corr,c}$ (A/m^2) of Steel	0.05
Galvanic Potential E_g (V/ECS)	- 0.855
Galvanic Current density i_g (A/m^2)	0.77
σ (S/m) conductivity of the electrolyte	6
e (m) thickness of the electrolyte	0.01
Anodic or cathodic radius (m)	0.025
K (C^{-1}.m^3) coefficient of proportionality	3.45 10^{-11}

4 Resolution

The above Laplace equation is solved over the electrolyte domain of the 2D geometry using adaptive meshing value, reaching a specified mesh quality as shown in Fig.3.

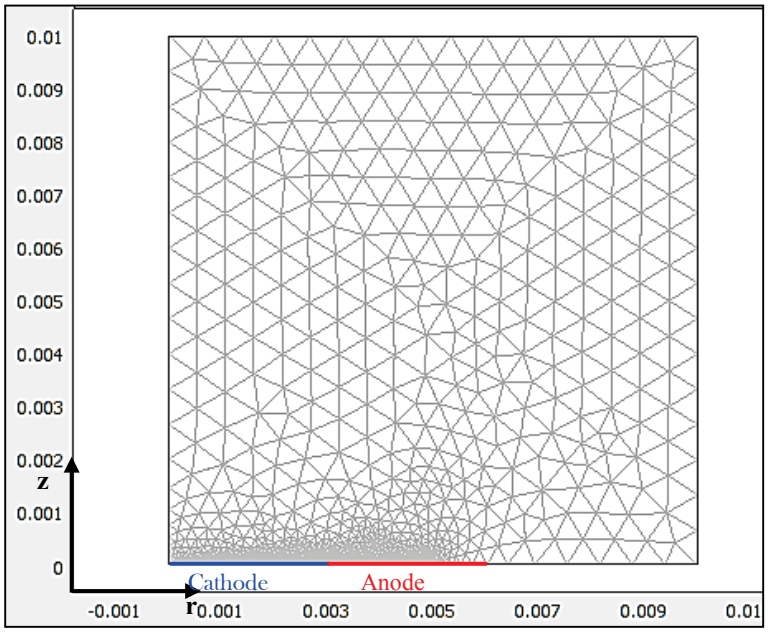

Fig. 3 – Model geometry with the corresponding meshing for the galvanic couple

5 Results

Simulation results show that the coupled numerical-analytical model associated with the mesh deformation has some capabilities to reproduce the phenomenon of corrosion or deposition of the metallic part.

The chemical reactions occurring on the metal interface exposed to the solution, lead to dissolution or deposit phenomenon. After solving the Laplace equation for the electric potential at time t = 0 and 3 days, the change in electrical potential over the electrolyte domain is shown in Fig. 4. This model can track the rate and the thickness of either the dissolution of anode with a displacement of the anode border downwardly to be occupied by the electrolyte (Fig.4.a) or the formation of an electro-deposited film (Fig.4.b).

The resolution of Laplace's equation with COMSOL enables us to calculate the distribution of electric potential and the normal and radial current density, for an electrolyte conductivity and time of immersion fixed.

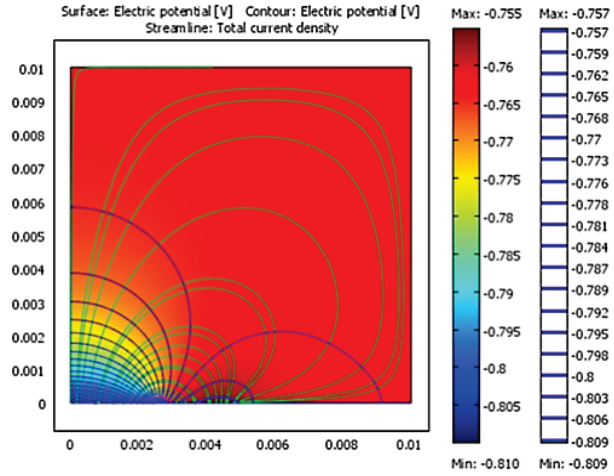

(a) t = 0s

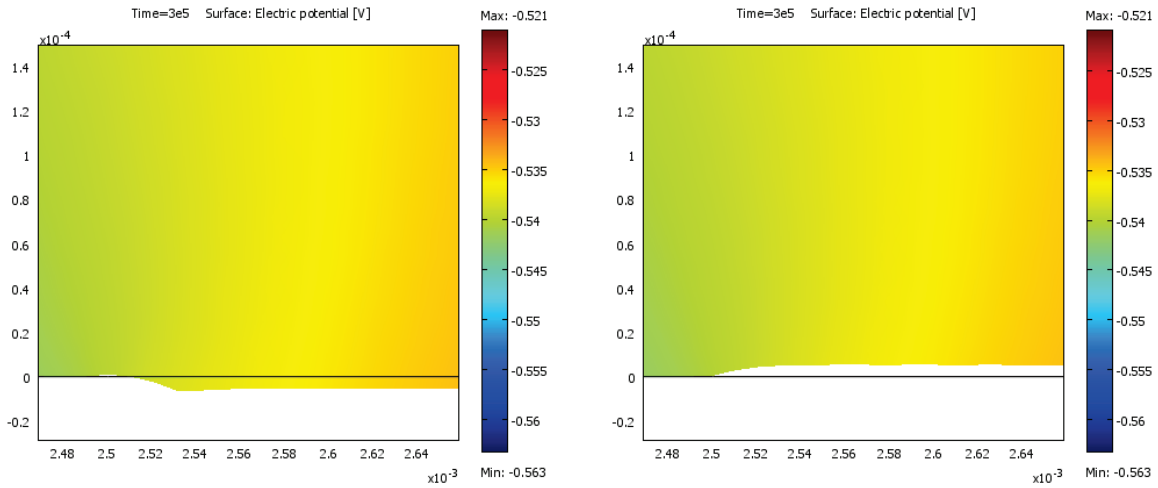

(b) **(c)**

Fig. 4 – Surface plot of steel/Al-Mg electric potential at a) 0s, b) and c) at 3. 10^5s and 0.06 S/m in the case of (b) dissolution and (c) deposition

The electric field which is the gradient of potential (in blue), is directed from anode towards cathode because of the potential difference, with a highest value near the junction and gradually decreases with distance from junction. The distribution of potential and current density as a function of normal distance z is shown in Figs. 5 and 6, respectively.

The shape of the local current density (Fig. 6) indicates that the i_z is higher at the junction between the two materials implying a large dissolution of Al-Mg and then i_z decreases away from the junction forming a pit. It is shown that, the potential distribution and the normal current density decreases by increasing the distance z between the surface of the galvanic couple and the point in the electrolyte where the measurement is performed according to the normal axis.

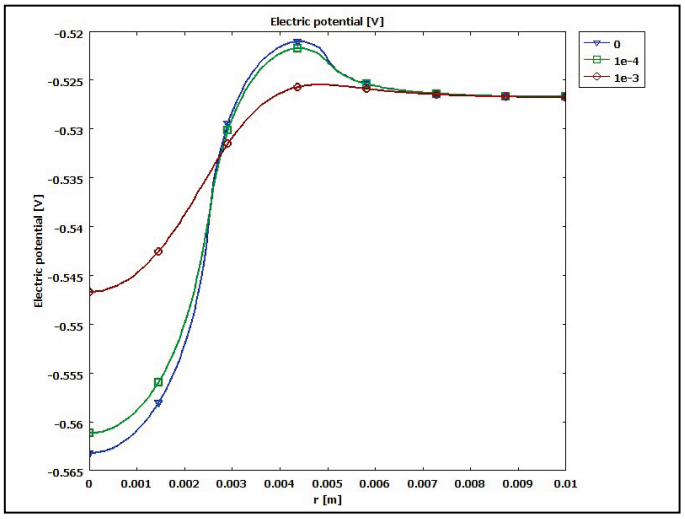

Fig. 5 – Distribution of electrical potential as a function of normal distance z

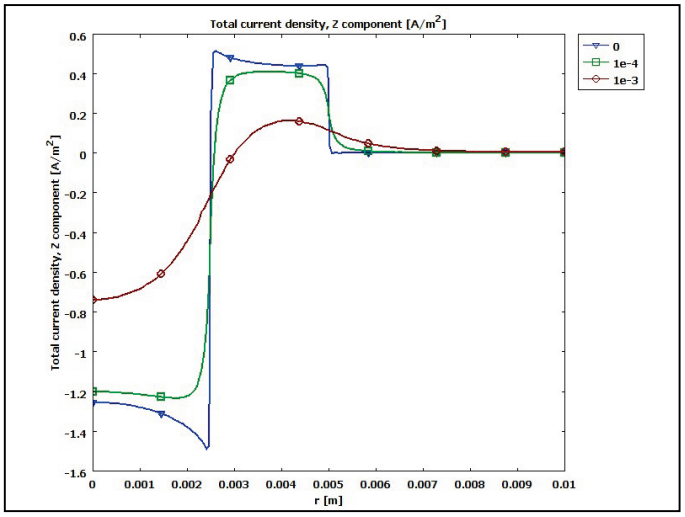

Fig. 6 – Distribution of current density as a function of normal distance z

The distributions of the profiles depth of the dissolution were shown in Fig. 7. The depth of the pit increases with the exposure time to the solution.

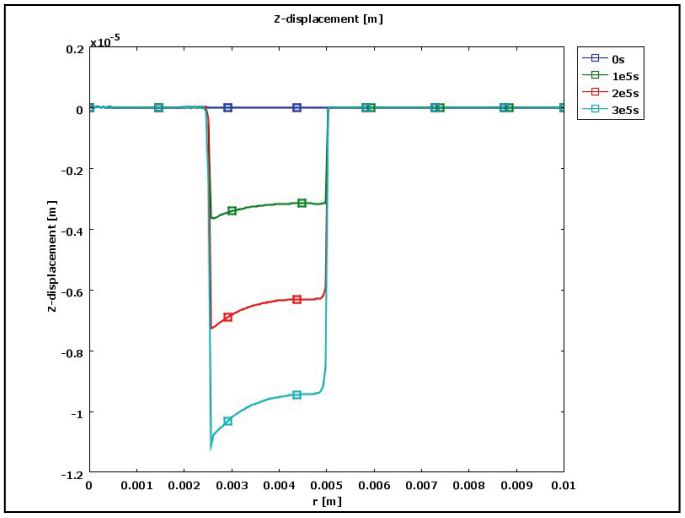

Fig. 7 – Depth profiles as a function of immersion time

The effect of the electrolyte conductivity on the depth profiles and the current density distribution is shown in Figs. 8 and 9, respectively. The results indicate that, the i_z distributions (Fig. 8) are larger in the diluted solution (low conductivity). The most active zone is at the junction between the anode and the cathode where a pit is developed. When increasing the electrolyte conductivity (electrolyte concentration) the total current density increase, in agreement with King et al. [32] and uniform depth of penetration is obtained (Fig. 9).

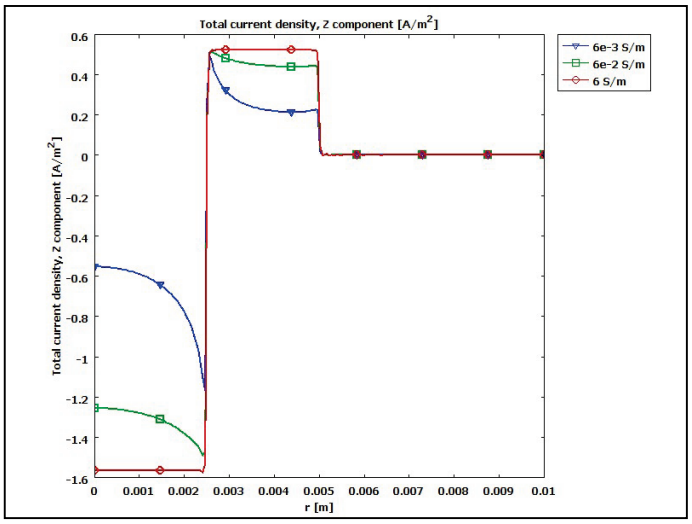

Fig. 8 – Normal current density distribution as a function of electrolyte conductivity after 6000s

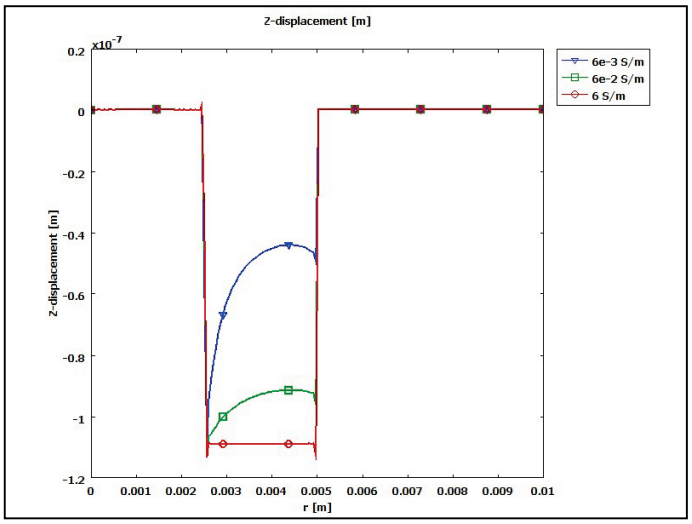

Fig. 9 – Depth profiles as a function of electrolyte conductivity after 6000 s

6 Conclusion

In this work the coupling of a numerical model with an analytical one has been developed in order to avoid meshing the anode and the cathode. The coupling with moving mesh technique is then easily performed and the border deformation is simulated accurately. The model could be used to simulate film deposition or metallic dissolution. The results obtained in both cases seem to be acceptable and qualitative results are satisfactory. In the future work the effect of the surface ration of the couple galvanic steel/Al-Mg by numerical modeling will determine.

REFERENCES

[1]- N. Murer, N. Missert, R. Buchheit, Towards the Modeling of Microgalvanic Corrosion in Aluminum Alloys: the Choice of Boundary Conditions. In: Proceedings of the COMSOL Users Conference Boston, 2008.

[2]- N. Murer, R. Oltra, B. Vuillemin, O. Néel, Numerical modelling of the galvanic coupling in aluminium alloys: A discussion on the application of local probe techniques. Corros. Sci. 52(1) (2010) 130-139. doi:10.1016/j.corsci.2009.08.051

[3]- C.R. Crowe, R.G. Kasper, Ionic Current Densities in the Nearfield of a Corroding Iron - Copper Galvanic Couple. J. Electrochem. Soc. 133(5) (1986) 879-887. doi:10.1149/1.2108755

[4]- K.B. Deshpande, Validated numerical modelling of galvanic corrosion for couples: Magnesium alloy (AE44)–mild steel and AE44–aluminium alloy (AA6063) in brine solution. Corros. Sci. 52(10) (2010) 3514-3522. doi:10.1016/j.corsci.2010.06.031

[5]- F. Thébault, B. Vuillemin, R. Oltra, K. Ogle, C. Allely, Investigation of self-healing mechanism on galvanized steels cut edges by coupling SVET and numerical modelling. Electrochim. Acta 53(16) (2008) 5226-5234. doi:10.1016/j.electacta.2008.02.066

[6]- F. Thébault, B. Vuillemin, R. Oltra, C. Allely, K. Ogle, Modeling bimetallic corrosion under thin electrolyte films. Corros. Sci. 53(1) (2011) 201-207. doi:10.1016/j.corsci.2010.09.010

[7]- D. Mizuno, Y. Shi, R.G. Kelly, Modeling of Galvanic Interactions between AA5083 and Steel Atmospheric Condition. In: Proceedings of the COMSOL Users Conference Boston, 2011.

[8]- C. Wagner, Theoretical Analysis of the Current Density Distribution in Electrolytic Cells. J. Electrochem. Soc. 98(3) (1951), 116-128. doi:10.1149/1.2778113

[9]- J.T. Waber, M. Rosenbluth, Mathematical Studies of Galvanic Corrosion: II. Coplanar Electrodes with One Electrode Infinitely Large and with Equal Polarization Parameters J. Electrochem. Soc. 102(6) (1955) 344-353. doi:10.1149/1.2430058

[10]- J.T. Waber, Mathematical studies of galvanic corrosion: VI. Limiting case of very thin films. J. Electrochem. Soc. 103(10) (1956) 567-570. doi:10.1149/1.2430158

[11]- E. McCafferty, Distribution of Potential and Current in Circular Corrosion Cells Having Unequal Polarization Parameters. J. Electrochem. Soc. 124(12) (1977) 1869-1878. doi:10.1149/1.2133178

[12]- J-M. Lee, Numerical analysis of galvanic corrosion of Zn/Fe interface beneath a thin electrolyte. Electrochim. Acta 51(16) (2006) 3256-3260. doi:10.1016/j.electacta.2005.09.026

[13]- R. Morris, W. Smyrl, Current and Potential Distribution in Thin Electrolyte Layer Galvanic Cells. J. Electrochem. Soc. 136(11) (1989) 3229-3236. doi:10.1149/1.2096430

[14]- F. Thebault, B. Vuillemin, R. Oltra, C. Allely, F. Dosdat, K. Ogle, Predictive Model for Cut-Edge Corrosion of Galvanized Steels. ECS Transactions 3(31) (2007) 343-353. doi:10.1149/1.2789240

[15]- J-B. Jorcin, C. Blanc, N. Pébère, B. Tribollet, V. Vivier, Galvanic Coupling Between Pure Copper and Pure Aluminum – Experimental Approach and Mathematical Model. J. Electrochem. Soc. 155(1) (2008) C46-C51. doi:10.1149/1.2803506

[16]- L. Lacroix, C. Blanc, N. Pébère, B. Tribollet, V. Vivier, Localized approach to galvanic coupling in an aluminium – magnesium system. J. Electrochem. Soc. 156(8) (2009) C259–C265. doi: 10.1149/1.3148833

[17]- K.B. Deshpande, Experimental investigation of galvanic corrosion: Comparison between SVET and immersion techniques. Corros. Sci. 52(9) (2010) 2819–2826. doi:10.1016/j.corsci.2010.04.023

[18]- K.B. Deshpande, Numerical modeling of micro-galvanic corrosion. Electrochim. Acta 56(4) (2011) 1737–1745. doi:10.1016/j.electacta.2010.09.044

[19]- J.X. Jia, G. Song, A. Atrens, Experimental measurement and computer simulation of galvanic corrosion of magnesium coupled to steel. Adv. Eng. Mater. 9(1-2) (2007) 65–74. doi:10.1002/adem.200600206

[20]- D. Trinh, P. Dauphin Ducharme, U. Mengesha Tefashe, J.R. Kish, J. Mauzeroll, Influence of edge effects on local corrosion rate of magnesium alloy/mild steel galvanic couple. Anal. Chem. 84(22) (2012) 9899–9906. doi:10.1021/ac3022955

[21]- N. Murer, N.A. Missert, R.G. Buchheit, Finite element modeling of the galvanic corrosion of aluminium at engineered copper particles. J. Electrochem. Soc. 159(6) (2012) C265–C276. doi:10.1149/2.102206jes

[22]- Y. Shi, R.G. Kelly, Experimental Evaluation and Modeling of Galvanic Interactions between Aluminum Alloy 7075-T6 and Noble Materials. ECS Transactions 41(25) (2012) 155-166. doi:10.1149/1.3697586

[23]- R. Oltra, A. Zimmer, C. Sorriano, F. Rechou, C. Borkowski, O. Néel, Simulation of pH-controlled dissolution of aluminium based on a modified Scanning Electrochemical Microscope experiment to mimic localized trenching on aluminium alloys. Electrochim. Acta 56(20) (2011) 7038-7044. doi:10.1016/j.electacta.2011.06.002

[24]- W. Sun, Optimal control of impressed cathodic protection system in ship building. Appl. Math. Model. 20(11)

(1996) 823-828. doi:10.1016/S0307-904X(96)00088-1

[25]- J.-F. Yan, T.V. Nguyen, R.E. White, R.B. Griffin, Mathematical modeling of the formation of calcareous deposits on cathodically protected steel in seawater. J. Electrochem. Soc. 140(3) (1993) 733-742. doi:10.1149/1.2056150

[26]- R. Radouani, Y. Echcharqy, M. Essahli, Numerical simulation of galvanic corrosion between carbon steel and low alloy steel in a bolted joint. Int. J. Corros. (2017) ID 6174904. doi:10.1155/2017/6174904

[27]- S. Fujimoto, Numerical Modeling for Corrosion. Electrochem. Soc. Interface 23(4) (2014) 45.

[28]- D. Boukhlef, D. Boughrara, H. Mohellebi, Modeling by Finite Elements Method of Nonlinear Conductivity in Corrosive Mediums. In: Proceedings of the International Conference on Mechanics, Materials, Mechanical Engineering and Chemical Engineering, Barcelona, Spain, (7-9 April 2015), pp. 203-210, ISSN: 2227-4596, ISBN: 978-1-61804-295-8.

[29]- H. Mohellebi, M. Féliachi, K. Srairi, Coupled 2D-Analytical and Finite Elements Analysis for the Eddy Current Computation. In: Proceedings of the Third International Workshop on Electric and Magnetic Field-Liège, Belgium, May 1996, pp. 339-341.

[30]- D. Schaefer, J. Doose, A. Rennings, D. Erni, Numerical Analysis of Propeller-induced Low-frequency Modulations in Underwater Electric Potential Signatures of Naval Vessels in The Context of Corrosion Protection Systems. In: Proceedings of COMSOL Conference in Stuttgart, 2011.

[31]- A. Ivanov, Simulation of electrochemical etching of silicon with COMSOL. In: Proceedings of the COMSOL Conference in Stuttgart, 2011.

[32]- A.D. King, J.S. Lee, J.R. Scully, Finite Element Analysis of the Galvanic Couple Current and Potential Distribution between Mg and 2024-T351 in a Mg Rich Primer Configuration. J. Electrochem. Soc. 163(7) (2016) C342-C356. doi:10.1149/2.0171607jes